The neural dynamics of familiar face recognition

Géza Gergely Ambrus [a, *], Daniel Kaiser [b, *], Radoslaw Martin Cichy [b, c, d], Gyula Kovács [a]

[a] *Institute of Psychology, Friedrich Schiller University Jena, Jena, Germany*

[b] *Department of Education and Psychology, Freie Universität Berlin, Berlin, Germany*

[c] *Berlin School of Mind and Brain, Humboldt-Universität Berlin, Berlin, Germany*

[d] *Bernstein Center for Computational Neuroscience Berlin, Berlin, Germany*

** These authors contributed equally to the study*

Abbreviated title: Neural dynamics of face recognition

Number of pages: 31

Number of figures: 5

Number of tables: 0

Words count Abstract: 201

Words count Introduction: 573

Word count Discussion: 684

Acknowledgements: The authors would like to thank Lisa-Celine Süllwold and Bettina Kamchen for their help in participant recruitment and data acquisition. This work was supported by grants from the Deutsche Forschungsgemeinschaft (KO3918/5-1, KA4683-2/1, CI241-1/1).

Conflicts of interest: The authors declare no competing financial interests.

Abstract

In real-life situations, the appearance of a person's face can vary substantially across different encounters, making face recognition a challenging task for the visual system. Recent fMRI decoding studies have suggested that face recognition is supported by identity representations located in regions of the occipito-temporal cortex. Here, we used EEG to elucidate the temporal emergence of these representations. Human participants (both sexes) viewed a set of highly variable face images of four highly familiar celebrities (two male, two female), while performing an orthogonal task. Univariate analyses of event-related EEG responses revealed a pronounced differentiation between male and female faces, but not between identities of the same sex. Using multivariate representational similarity analysis, we observed a gradual emergence of face identity representations, with an increasing degree of invariance. Face identity information emerged rapidly, starting shortly after 100ms from stimulus onset. From 400ms after onset and predominantly in the right hemisphere, identity representations showed two invariance properties: (1) they equally discriminated identities of opposite sexes and of the same sex, and (2) they were tolerant to image-based variations. These invariant representations may be a crucial prerequisite for successful face recognition in everyday situations, where the appearance of a familiar person can vary drastically.

Significance Statement

Recognizing the face of a friend on the street is a task we effortlessly perform in our everyday lives. However, the necessary visual processing underlying familiar face recognition is highly complex. As the appearance of a given person varies drastically between encounters, for example across viewpoints or emotional expressions, the brain needs to extract identity information that is invariant to such changes. Using multivariate analyses of EEG data, we characterize how invariant representations of face identity emerge gradually over time. After 400ms of processing, cortical representations reliably differentiated two similar identities (e.g., two famous male actors), even across a set of highly variable images. These representations may support face recognition under challenging real-life conditions.

Introduction

Efficient face recognition is a key ability in human's everyday lives, and many studies have investigated its underlying neural mechanisms (Gobbini and Haxby, 2007; Duchaine and Yovel, 2015). Recently, much progress has been made in spatially pinpointing the neural correlates of face recognition by advances in multivariate classification techniques for fMRI data (Anzellotti and Caramazza, 2014). These techniques have allowed researchers to decode face identity from different regions of the face processing network, such as from the fusiform face area (FFA; Gilaie-Dotan and Malach, 2007; Nestor et al., 2011; Goesaert and Op de Beeck, 2013; Verosky et al., 2013; Anzellotti et al., 2014; Axelrod and Yovel, 2015; Weibert et al., 2016), the anterior temporal lobe (ATL; Kriegeskorte et al., 2007; Nasr and Tootell, 2012; Anzellotti et al., 2014) or from a larger network extending from early visual areas towards the inferior frontal gyrus (Visconti Di Oleggio Castello et al., 2017).

The temporal emergence of face identity representations, however, remains relatively unexplored. Most of our knowledge on the temporal dynamics of face recognition stems from EEG and magnetoencephalography (MEG) studies employing traditional, univariate analyses on temporally confined ERP/MEP components. Across these studies, the components associated with face recognition vary substantially: Several reports have linked face recognition to the P100 and N170 components (Debruille et al., 1998; Heisz et al., 2006; Caharel et al., 2009; Rousselet et al., 2009; Liu et al., 2013), others have stressed the role of the later N250 and N400 components (Bentin and Deouell, 2000; Schweinberger et al., 2002; Huddy et al., 2003; Tanaka et al., 2006; Curran and Hancock, 2007; Gosling and Eimer, 2011; Jin et al., 2012).

So far only three studies have used multivariate pattern analysis (MVPA) to evaluate the temporal dynamics of face identity processing (Nemrodov et al., 2016, 2018; Vida et al., 2017). All three investigated the temporal emergence of identity representations across changes in emotional expression, revealing that identity representations emerge relatively early within the first 200ms after stimulus onset.

However, these previous studies suffer from two critical shortcomings. First, they used unfamiliar faces, whose processing is assumed to be markedly different from the processing of familiar faces, as reflected both in behavioral performance (Johnston and Edmonds, 2009) and neural activations (Natu and O'Toole, 2011). Second, variability across images of the same identity was very limited, leaving it unclear how their results generalize to everyday face recognition where individual encounters with highly-variable, "ambient" face images give rise to drastic visual differences (Mike Burton, 2013; Young and Burton, 2017; Kramer et al., 2018).

In the current EEG study, we provide a temporal characterization of face identity processing, which eliminates both shortcomings: First, we used images of four celebrities, who were highly familiar to the participants (Fig. 1A). Second, for each identity, we used 10 "ambient" images (Jenkins et al., 2011), which varied substantially in a range of properties, such as viewpoint, lighting, and expression.

Using representational similarity analysis (RSA; Kriegeskorte and Kievit, 2013), we show that the earliest representations of facial identity emerge shortly after 100ms post-stimulus and most robustly in posterior electrodes. Later representations, emerging from 400ms onwards and in electrodes over right occipito-temporal cortex, contained identity information for faces of the same sex and were invariant to image-based properties. Our results suggest that familiar face recognition is supported by fine-grained neural representations in the face processing network,

98 where identity information over time becomes increasingly invariant to other visual and

99 conceptual properties of the face.

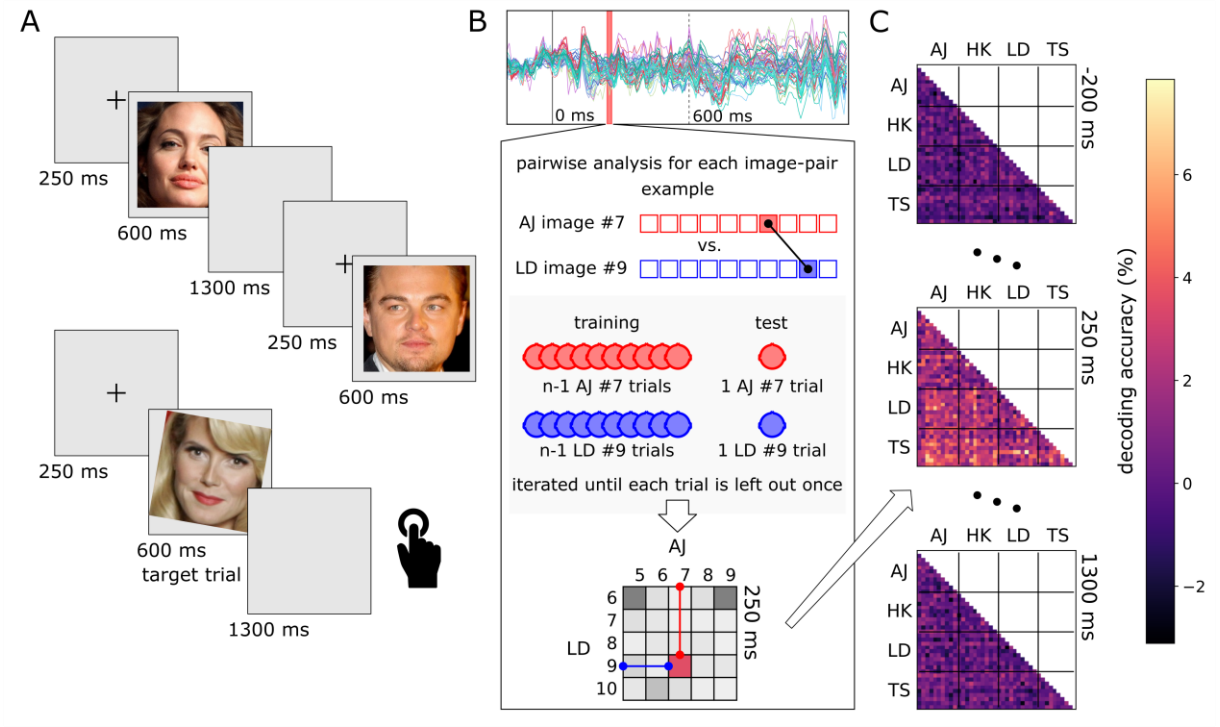

Figure 1. Design and Analysis Approach. A. Trial structure and stimulus examples. Stimuli were "ambient", face-cropped images of four highly recognized celebrities (Angelina Jolie (AJ), Heidi Klum (HK), Leonardo DiCaprio (LD), Til Schweiger (TS))[1]. Each trial started with a fixation cross (250ms), followed by the stimulus image (600ms) and a blank screen (1300ms). Target trials containing a tilted stimulus (illustrated on the bottom) were included to ensure that participants maintained attention. B. The logic of the multivariate pattern analysis. Top: A representative ERP recording from one participant. EEGs were segmented between -200 to 1300ms relative to stimulus onset. Bottom: For each time point separately, linear classification analyses were performed for each combination of individual images, using a leave-one-trial-out scheme. This procedure resulted in a 40×40 matrix (i.e., 10 images for each of the 4 identities) of decoding accuracies at each time point. C. Representational dissimilarity matrices (RDMs) showing pairwise decoding accuracies at -200, 250 and 1300ms relative to stimulus onset.

[1] Image credits: File:Angelina Jolie at Davos crop.jpg. (2014, April 23). *Wikimedia Commons, the free media repository*. Retrieved 15:17, May 1, 2018 from https://commons.wikimedia.org/w/index.php?title=File:Angelina_Jolie_at_Davos_crop.jpg&oldid=122076100. Creative Commons Attribution-Share Alike 3.0 Unported license.
File:LeonardoDiCaprioNov08.jpg. (2018, January 20). *Wikimedia Commons, the free media repository*. Retrieved 15:18, May 1, 2018 from

Methods

Participants

Twenty-six healthy participants (6 male), with an average age of 25 years (SD = 5.0) took part in the study in exchange for partial course credits or monetary compensation. The experiment was conducted in accordance with the guidelines of the Declaration of Helsinki, and with the approval of the ethics committee of the University of Jena. Written informed consent was acquired from all participants.

Stimuli

The stimuli were ambient, color photographs two female (Angelina Jolie, AJ; Heidi Klum, HK) and two male (Leonardo DiCaprio, LD; Til Schweiger, TS) celebrities. We selected these celebrities based on a pilot survey where we collected familiarity ratings across a range of well-known celebrities in Germany. For each identity, ten images were selected from a pool of web-scraped photographs, pre-screened for quality. Stimulus images were cropped to a rectangle centered on the inner features of the face (see Fig. 1A). To ensure substantial variation across images depicting the same identity, we selected images that minimized the structural similarity index (SSIM; Wang et al., 2004) among images of the same identity, while maximizing it among images of identities of the same sex; this was achieved by using random combination sorting with 100,000 iterations per sex category. The resulting mean SSIM values were: LD: 0.387, TS: 0.378, LD vs TS: 0.355; AJ: 0.379, HK: 0.371, AJ vs HK: 0.337. Stimuli were presented centrally on a uniform gray background

https://commons.wikimedia.org/w/index.php?title=File:LeonardoDiCaprioNov08.jpg&oldid=281183411. Creative Commons Attribution-Share Alike 3.0 Unported license.
These images were not part of the original stimulus set.

on a TFT display (1680 × 1050 pixel resolution, refresh rate 60 Hz). The experiment was written in Psychopy (Peirce, 2008).

Experimental procedure

A total of 1760 trials (1600 non-target and 160 target) were presented in 40 runs, each containing the ten images of the four identities once, in a pseudo-random order (with the constraint that the same identity was never repeated in two consecutive trials). Thus, photos of one identity were seen 400 times, so that a given image of a given identity was presented 40 times during the experiment. Each trial started with a fixation cross (250ms), followed by the stimulus image (600ms, subtending a visual angle of 4.4° in diameter) and finally a blank display (1300ms). Short breaks were provided after every 10 runs, but the run boundaries were not indicated otherwise. There were four target-trials in each run, where the image was rotated 10 degrees clockwise or anticlockwise. Participants were instructed to press the space bar when they saw a target image (the overall detection accuracy was at 99.52 ± 0.67%). These target trials served to ensure that the participants maintained their attention, and were not included in the analysis. An average experimental session lasted 81.5 (±5.3) minutes.

At the beginning of each experiment, prior to mounting the electrode caps, participants were presented images of the four identities and were asked to name them. All our participants were able to name all four celebrities correctly. The images of this initial familiarity-testing phase were not part of the later EEG experiment. After the EEG recording, participants were asked to rate their familiarity with the identities on a 7-point scale. Mean ratings were generally high (AJ: 6.12, HK: 6.30, LD: 6.15, TS: 6.11) and not statistically different for the four identities ($F[3,75] = 0.243$, $p = 0.866$).

EEG recording and preprocessing

The EEG was recorded in a dimly lit, electrically shielded, and sound–attenuated chamber. The distance between the eyes and the computer screen was set to 96 cm via a chin rest. The electroencephalogram (EEG) was recorded with a 512 Hz sampling rate (bandwidth: DC to 120 Hz) using a 64-channel Biosemi Active II system. Electrooculogram (EOG) was recorded from the outer canthi of the eyes and from above and below the left eye.

The preprocessing pipeline was implemented in MNE-python (Gramfort et al., 2013, 2014). EEG was notch-filtered at 50 Hz, band-pass filtered between 0.1 and 70 Hz, segmented from -200 to 1300ms relative to stimulus onset, and baseline corrected with respect to the first 200ms. Artefact rejection was carried out using the "Autoreject" algorithm (Jas et al., 2017). The resulting data was downsampled to 100Hz to increase signal-to-noise ratio in the multivariate analyses (Grootswagers et al., 2017).

Event-related potentials

To test for the presence of identity-related information within the conventional ERPs we averaged data across repetitions for each facial identity, electrode and participant separately. Next, we created grand-averages of these data across six regions of interests, corresponding to the left and right anterior (Fp, AF, F, FC), central (FT, TP, C, T) and posterior occipito-temporal electrodes (PO, P, O, I). The central electrodes (Fpz, AFz, Fz, FCz, Cz, CPz, Pz, POz, Oz, Iz) were included in both the left and the right clusters; this was done to maintain sufficient electrode counts for the multivariate analyses (see below). For reasons of consistency, the same electrode clusters were used in both analyses. The posterior clusters included the electrodes typically yielding the largest face-sensitive N170 components (Rossion and Jacques, 2008). First, we tested for identity selectivity by using a one-way repeated measures ANOVA with identity (4) as a factor. Second,

we averaged the two female and two male face elicited ERPs and performed a paired t-test for testing sex-specific differences. Third, we tested if the ERPs differed for the two identities within the same sex by comparing the ERPs for the two female as well as for the two male identities with each other in t-tests.

Representational Similarity Analysis

To model the neural organization of face representations, we performed a representational similarity analysis (RSA; Kriegeskorte et al., 2008) on the EEG data. In this analysis (Fig. 1B/C), the neural dissimilarity between all pairs of face images (i.e., between all 40 individual images), was modeled as a function of different predictor matrices (see below).

Neural dissimilarity. Neural dissimilarity was extracted by performing a linear classification analysis, where pairwise decoding accuracies were used as a measure of representational dissimilarity. Classification analysis was carried out using the CoSMoMVPA toolbox (Oosterhof et al., 2016). Linear-discriminant-analysis (LDA) classifiers were trained and tested on response patterns across all 64 electrodes, separately for each time point across the epoch (downsampled to 100 Hz, i.e., with a 10ms resolution) and separately for each pair of images. Training and testing was done in a leave-one-out scheme (Fig. 1B): classifiers were trained on all but one trials for each of the two conditions, and tested on the left-out trials. This procedure was repeated until each trial was left out once, and classification accuracy was averaged across these repetitions. Pairwise classification time-courses were smoothed with a 30ms (i.e., 3 consecutive time points) averaging window (Kaiser et al., 2016). This classification analysis led to one representational dissimilarity matrix (RDM; 40×40 entries, with empty diagonal) for each time point (Fig. 1C).

Modelling neural dissimilarity. To model the neural dissimilarity, we created four categorical predictor RDMs. Each predictor RDM covered 40×40 elements, and contained zeros

where the entries represented comparisons of similar images (i.e., similar on the dimension of interest, see below) and ones, where the entries reflected comparisons of dissimilar images. To quantify correspondence between the predictor RDMs and the neural RDMs, we unfolded the lower off-diagonal elements of the matrices into two vectors (i.e., the diagonal of both matrices was discarded) and correlated the vectors using Spearman's correlation coefficients. These correlations were computed separately for each time point, leading to a time series of correlations that reflected the correspondence of the neural data and the predictor. Individual-participant correlations were Fisher-transformed.

Modelling identity Information. For assessing differences between the four identities, all comparisons within a given identity (e.g., two images of AJ) were marked as similar (0) and all comparisons between two identities (e.g., an image of AJ and an image of TS) were marked as dissimilar (1) (Fig. 3A).

Modelling sex information. For assessing differences between face sexes, all comparisons within the same sex (e.g., an image of AJ and an image of HK) were marked as similar (0), and all comparisons between the different sexes (e.g., an image of AJ and an image of TS) were marked as dissimilar (1). To avoid confounding sex information with identity information, all comparisons within the same identity (e.g., two different images of AJ) were excluded from this analysis (as including these comparisons would overestimate the effect of sex) (Fig. 3C).

Modelling identity information between and within sexes. To uncover interactions between sex and identity processing, we constructed identity predictor RDMs that only covered all comparisons across the sexes or within one sex. The between-sex RDM was generated from the identity predictor matrix by removing all comparisons of two different identities of the same sex (e.g., an image of AJ and an image of HK), leaving only comparisons within identity (0) and

between identities of the opposite sex (1). The within-sex RDM was generated from the identity predictor matrix by removing all comparisons of two identities of different sexes (e.g., an image of AJ and an image of TS), leaving only comparisons within identity (0) and between identities of the same sex (1) (Fig. 3E). Note that this within-sex analysis tests for identity representations in more thorough way: by removing between-sex comparisons, the more pronounced differences between faces of the opposite sex (due to face sex, and due to visual differences) are eliminated.

Sensor-space RSA. To track representational organization across electrode space, we additionally repeated the RSA across the six electrode clusters also used in the ERP analysis (see above). Including central electrodes (Fpz, AFz, Fz; FCz, Cz, CPz; Pz, POz, Oz, Iz) in both left- and right-hemispheric clusters yielded electrode counts of 9, 15, and 13, for the anterior, central, and posterior clusters, respectively. All technical details of the cluster-specific RSAs were identical to the analysis using all available electrodes.

Controlling for image similarity. To quantify similarity on the image level, we computed pixel similarities for all pairs of images. Each image (220×220 pixels in 3 color layers) was first unfolded into a vector; these vectors were then correlated for each pair of images. A pixel RDM was generated by using 1 – correlation as the dissimilarity measure. As the pixel RDM explained some variance in the face identity RDM (R^2=.06), neural identity representations could in principle partly reflect pixel similarities. Hence, we used a partial correlation approach (Cichy et al., 2017; Groen et al., 2018), where we repeated the key analyses while removing the pixel RDM by partialing it out. This analysis revealed representations of face identity that are invariant to pixel-based image similarities.

Statistical testing

To identify significant effects across time, we used a threshold-free cluster enhancement procedure (Smith and Nichols, 2009)with default parameters. Multiple-comparison correction across time was based on a sign-permutation test (with null distributions created from 10,000 bootstrapping iterations) as implemented in CoSMoMVPA (Oosterhof et al., 2016). The resulting statistical maps were thresholded at $Z>1.64$ (i.e., $p<.05$, one sided against zero).

Results

Event-related potentials reflect face sex, but not face identity

Following traditional EEG studies on face perception, we first performed a univariate ERP analysis across six electrode clusters (Fig. 2). ERPs were different for the four identities primarily in the bilateral posterior electrode clusters (main effect of identity in a four-way ANOVA, Fig. 2E/F, purple line) starting from 100ms for the left and 120ms for the right hemisphere (Fig. 2), remaining significant throughout the length of the epoch. The other electrode clusters showed weaker and less temporally persistent differences (A-D). The difference between identities however originated from the significantly different ERPs for female and male faces from 190ms (left) and 150ms (right), throughout the length of the epoch. By contrast, within-sex comparisons led to no significant results at any of the time-points over either of the electrode clusters. These results support prior studies showing that ERP signals more prominently reflect face sex than face identity (Mouchetant-Rostaing et al., 2000; Freeman et al., 2010). In the following we applied multivariate pattern analysis to further probe the emergence of identity information with higher sensitivity.

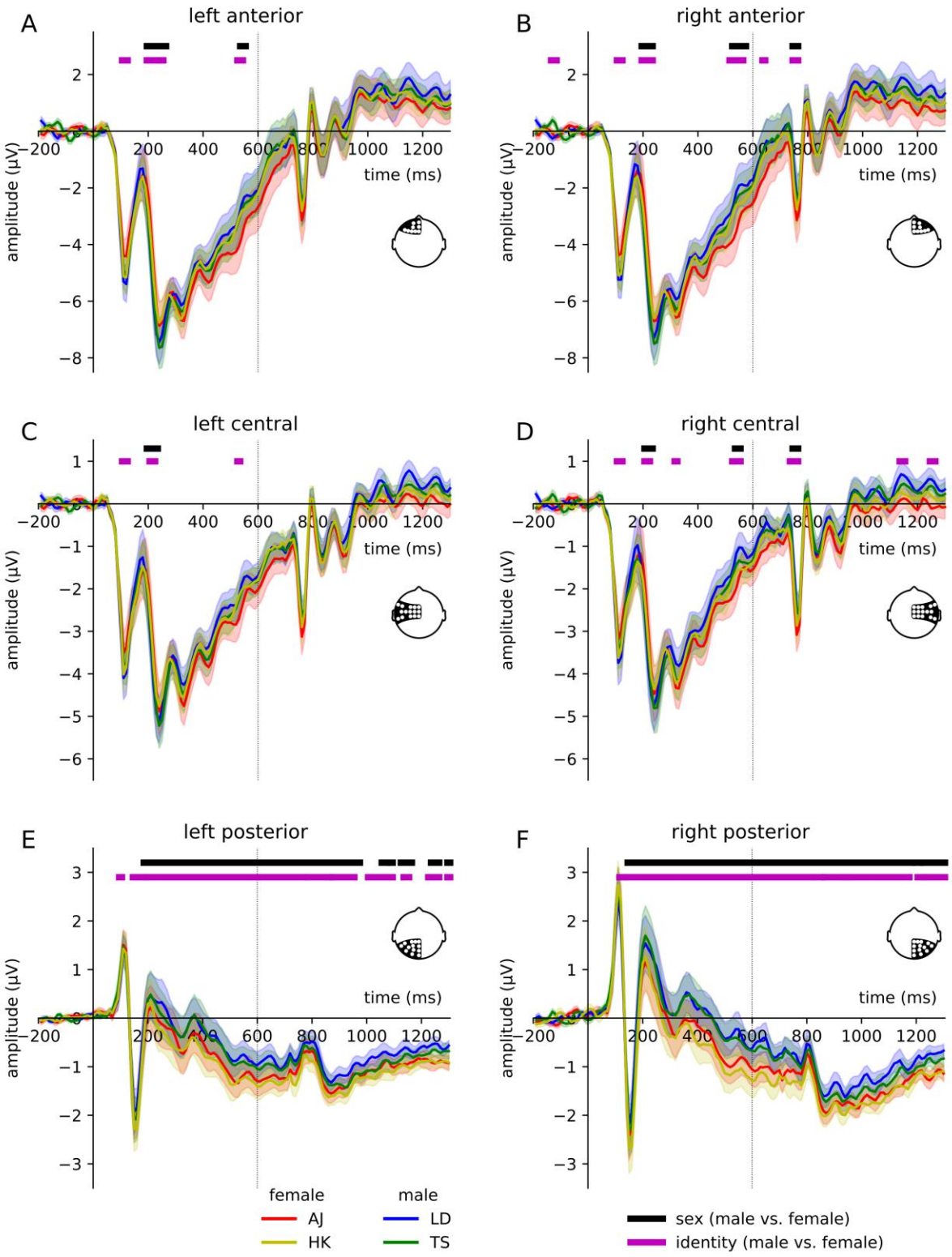

Figure 2. ERP Results. Grand-average ERPs were significantly differed across the four identities (purple significance markers), particularly in the posterior electrode clusters (E, F). This effect

was driven by a pronounced difference between male and female faces (black significance markers). Identities of the same sex were not discriminable from ERP responses in any of the clusters, suggesting that ERPs primarily reflect face sex, rather than face identity. Red, blue, yellow and green show the average ERPs for the four celebrities. Horizontal lines denote statistical significance ($p<0.05$, FDR-corrected for multiple comparisons). Shaded ranges denote standard errors of the mean.

Tracking the emergence of face identity representations

To reveal identity information in the EEG signals, we generated an identity predictor RDM, which reflected the 40 images' dissimilarity in identity (Fig. 3A). We then correlated the neural RDM with this identity RDM separately at every time point. This analysis revealed significant correlations from 110ms onwards, peaking at around 410ms (peak $t[25]=5.97$) and lasting across the whole epoch (Fig. 3B), suggesting rapidly emerging and long-lasting face identity information in the signal.

Our stimulus set contained faces of both sexes, and faces within the same sex share more visual and conceptual properties than faces of opposite sexes (O'Toole et al., 1998). To determine whether such sex differences could be retrieved from the EEG signals, we correlated the neural RDM with a sex predictor RDM separately at every time point (Fig. 3C). This sex predictor RDM only contained between-identity comparisons, so that this analysis reflected face sex independently of identity. We found significant sex information from 140ms to 680ms, peaking at 270ms (peak $t[25]=4.39$) (Fig. 3D). This indicates that the early EEG signals also contain reliable differences between sexes, emerging at a similar time point as identity-specific information but decaying more rapidly.

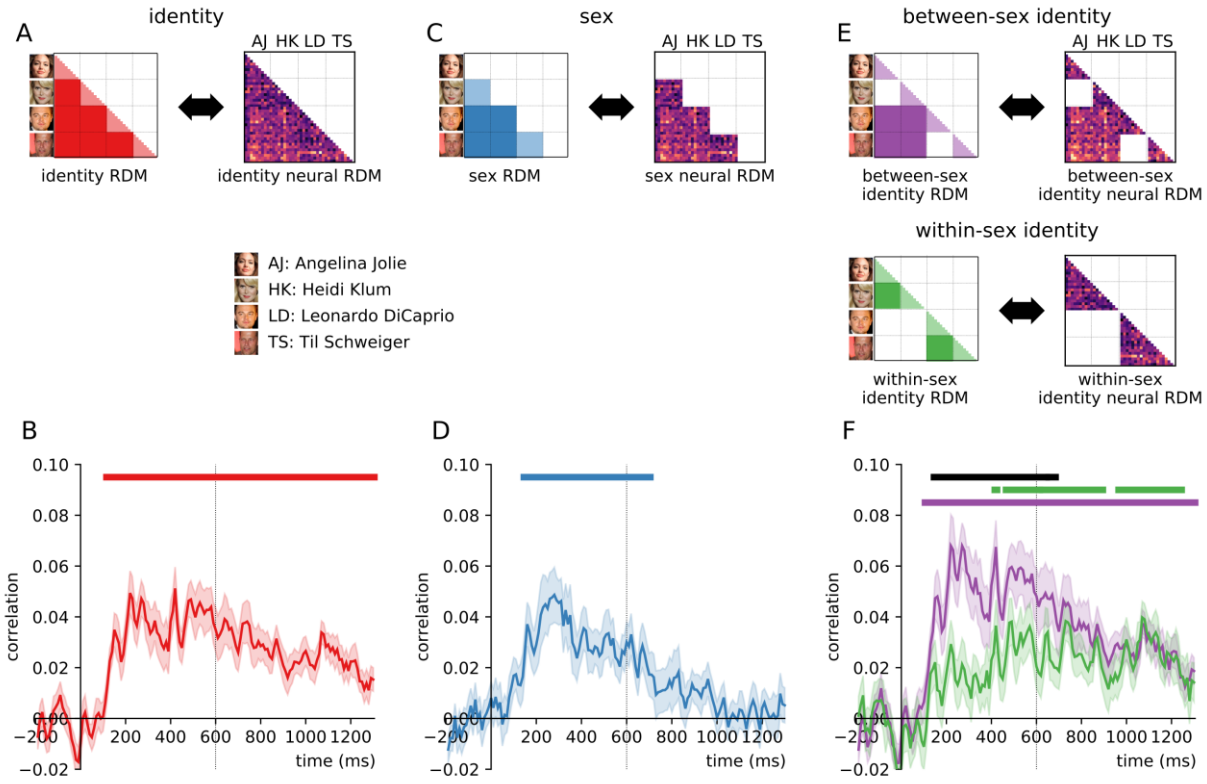

Figure. 3: RSA Results. To reveal identity-specific representations, we modeled the representational organization obtained from EEG signals with different predictor matrices (A, C, E). We observed temporally persisting identity information starting from 110ms after stimulus onset (A, B). Similarly, we found strong sex information in the neural organization, emerging between 140ms and 680ms (C, D). Tracking identity information for faces of same and opposite sexes revealed that identity information for same-sex faces was relatively delayed, emerging only after 400ms (E, F). Early identity information was significantly reduced for between-sex comparisons (black significance markers), suggesting that early identity coding partly relies on differences in face sex. Horizontal lines denote statistical significance ($p<0.05$, corrected for multiple comparisons). Shaded ranges denote standard errors of the mean.

272

273 The presence of sex information in the signal suggests that identity information may be
274 processed differently as a function of the sex of the face. Specifically, as faces of the same sex are
275 more similar in various aspects (including their visual appearance), discriminating between the

four facial identities may overestimate the amount of genuine identity information in the signal. We thus split our analysis into comparisons between faces of opposite and of the same sex by correlating the neural RDMs with two separate predictor RDMs (Fig. 3E).

For one of these predictor RDMs ("between-sex") we only included comparisons between the two sexes, while for the other RDM ("within-sex") we only included comparisons within the same sex. We observed strong identity information for opposite-sex faces that could be retrieved from as early as 100ms until the end of the epoch and peaking at 260ms (peak t[25]=7.40). Identity information, however, differed when restricting the analysis to within-sex comparisons: it emerged significantly later, at around 400ms, and peaked at 1,050ms (peak t[25]=5.97) (Fig. 3F). When directly comparing identity information for the between- and within-sex comparisons, we found significantly higher identity information for the between-sex analysis between 140ms and 660ms. This suggests that early identity representations partly reflect differences in face sex. By contrast, after 660ms, face sex did not influence identity representations, suggesting the emergence of identity representations that are invariant to commonalities and differences across the two sexes.

Face identity information predominantly originates from right posterior sources

As highlighted by previous neuroimaging studies (Rossion et al., 2003, 2012) (for a recent review see Yovel, 2016), and evident from our univariate results (see above), face-selective responses are strongest over right posterior electrodes. Using response patterns across the whole scalp may therefore partly obscure face identity information in the multivariate analyses. We thus repeated the RSA separately for each of the six electrode clusters used in the univariate analysis, expecting the strongest identity information in the right posterior cluster (Fig. 4).

For the posterior electrode clusters we found the most pronounced identity information, and a marked difference between hemispheres. In the left posterior cluster, four-way identity information (where sex may contribute to identity encoding) emerged from 120ms post-stimulus onset and peaked at 560ms (peak t[25]=4.85) (Fig. 4E). However, restricting the analysis to within-sex comparisons abolished identity information over this electrode cluster in the signal entirely. Similarly, in the right posterior cluster (Fig. 4F) we found robust four-way identity information, starting from 110ms after stimulus onset and peaking at 230ms (peak t[25]=4.81). Crucially however, the right posterior cluster also showed reliable within-sex identity information throughout the epoch, emerging at the same time, after 110ms and peaking around 530ms (peak t[25]=5.40). This result suggests that signals recorded from electrodes close to the typically face-selective ERP recording sites of the right hemisphere contain widespread identity information, even when visual and conceptual properties are more robustly controlled for.

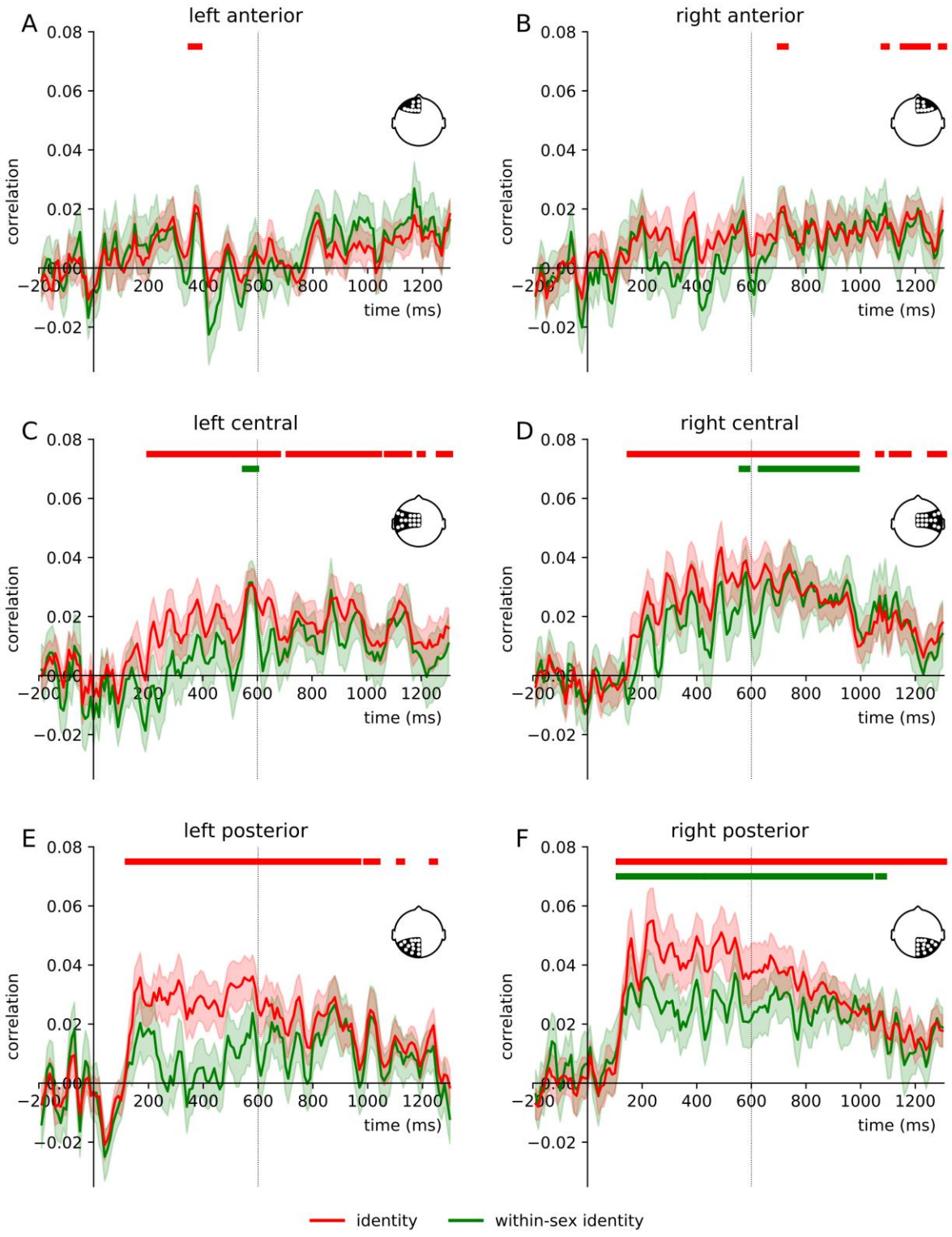

Figure 4. Sensor-space RSA Results. When repeating the RSA for the six electrode clusters used in the ERP analysis, we found strongest identity information in the posterior clusters (E/F). This identity information was lateralized to the right hemisphere: In the right central and posterior

electrode clusters (D/F), we observed significant within-sex identity information, with an early onset (110ms) in the right posterior cluster. The corresponding left-hemispheric clusters (C/E) only yielded identity information when also the between-sex comparisons were included. The anterior clusters (A/B) did not yield substantial identity information. Horizontal lines denote statistical significance ($p<0.05$, corrected for multiple comparisons). Shaded ranges denote standard errors of the mean.

312

313 The left central cluster (Fig. 4C) primarily showed four-way identity information, emerging
314 slightly later as compared to the posterior cluster, after 200ms, peaking at 560ms (peak
315 t[25]=5.10). By contrast, the right central cluster not only yielded four-way identity information
316 (from 150ms, peaking at 480ms, peak t[25]=4.97), but also within-sex identity information,
317 emerging later than that of the posterior cluster, after 550ms and peaking at 1,100ms (peak
318 t[25]=3.11).

319 Signals recorded from the two anterior clusters did not yield substantial identity
320 information (Fig. 4A/B), suggesting that identity information primarily originates from sources in
321 visual cortex.

322

323 ## Late representations of face identity are invariant to image properties

324 Our stimulus set was constructed to mirror natural variations across different encounters with a
325 familiar person. This was achieved by selecting stimuli that ensured a high degree of variability
326 within each identity (see above), so that image-based stimulus properties are unlikely to account
327 for the emergence of identity information. To explicitly rule out this possibility, we performed a
328 control analysis, where we additionally modeled image-based similarities between stimuli. This
329 was done by constructing pixel RDMs, which reflected the images' dissimilarity in pixel values;

these pixel RDMs were partialled out in the subsequent analysis. We focused the control analysis on the within-sex comparison, which forms the most robust test of face identity representations, and on the two electrode configurations where it was most robustly found (all electrodes and right posterior electrodes).

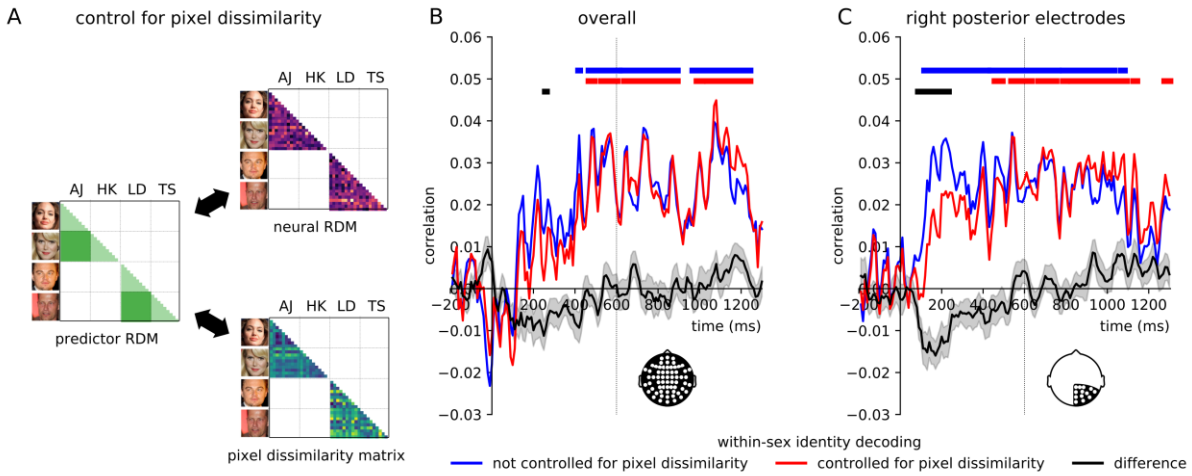

Figure 5. Controlling for Image Similarity. In a partial correlation analysis, we tracked within-sex identity information while controlling for the images' pixel dissimilarities (A). When using data from all electrodes, removing pixel dissimilarities did not significantly impact identity information (B). For the right posterior cluster, where early within-sex identity information was found in previous analysis (Fig. 4F), controlling for pixel dissimilarity had a significant impact (C): early identity information (90-230ms) was significantly reduced when controlling for pixel dissimilarity, whereas later identity information was not impacted and remained significant from 460ms after onset. These results suggest that later representations of face identity are invariant to image-based properties. Horizontal lines denote statistical significance ($p<0.05$, corrected for multiple comparisons). Shaded ranges denote standard errors.

In the analysis using all electrodes, we found no modulation of identity information after removing the pixel RDM (Fig. 5B). By contrast, when focusing on the right posterior cluster, we found a modulation of identity information when controlling for image-based similarity (Fig. 5C).

Early within-sex identity information, emerging between 90ms and 230ms was significantly reduced when controlling for pixel dissimilarity. By contrast, later within-sex identity information (from 460ms) emerged independently of image-based properties. Together, these results suggest that later representations of face identity are robust to image-based changes, but genuinely reflect face identity. These neural representations might thus be a crucial prerequisite for efficient face recognition across visually different encounters with a person.

Discussion

In the current study, we applied representational similarity analysis to EEG signals to investigate the neural dynamics of familiar face recognition. Our results show that face identity can be rapidly recovered from EEG response patterns, even with highly variable, "ambient" face stimuli (Jenkins et al., 2011). In more fine-grained analyses, we uncovered a gradual emergence of face identity coding: Early identity information is modulated by face sex and by visual image properties. By contrast, later identity information, emerging after 400ms and primarily in the right hemisphere, is unaffected by these factors. This finding suggests that after 400ms representations genuinely reflect face identity. These later representations may be the basis for real-world face recognition, allowing the identification of an individual across different encounters and against similar-looking other faces.

In everyday life, the facial appearance of a single person can be highly variable. This variability makes it challenging to match an individual encounter with a face to an identity representation stored in memory (Bruce et al., 1999; Clutterbuck and Johnston, 2002; Jenkins et al., 2011; Andrews et al., 2015). The invariant identity representations revealed here are ideal for extracting face identity from different encounters, as they discriminate identities of the same sex,

361 across variations in visual properties. The late emergence of such representations is compatible
362 with the involvement of conceptual identity representations in the medial and anterior temporal
363 cortices (Quiroga et al., 2005; Mormann et al., 2008); linking our EEG results with functional
364 neuroimaging data (Cichy et al., 2014, 2016) could directly test this possibility in the future.

365 How do these seemingly late identity representations support rapid face recognition in
366 the wild? While these representations are useful under great variability and in the presence of
367 distracting face information, face recognition is sometimes easier than this: In real-life situations,
368 we often know which person to expect, which visual properties are diagnostic of him or her, and
369 where the person likely shows up. Under such conditions, motor responses in face recognition
370 tasks can be faster than 400ms (Besson et al., 2017). This observation suggests that face identity
371 can sometimes be inferred from earlier representations that do not need to be highly invariant.
372 Future studies could thus test whether different representational stages are crucial for face
373 recognition under varying demands.

374 Our study revealed a pronounced right-hemispheric lateralization of identity information:
375 face identity information was strongest in electrodes over the right, as opposed to the left, visual
376 cortex. Specifically, only signals recorded over right occipito-temporal cortex contained identity
377 information which is invariant to both face sex and image-based properties. This right-lateralized
378 topography is consistent with sources in the visual face processing network that has a strong right-
379 hemispheric lateralization (Axelrod and Yovel, 2015; Yovel, 2016). Interestingly, neuroimaging
380 work showed that specifically right-hemispheric activations predict behavioral performance in
381 familiar face recognition (Weibert and Andrews, 2015), suggesting that these identity
382 representations could play an important role in face recognition. However, this notion has to be

383 explicitly tested in the future, as caution needs to be applied when inferring cortical sources from
384 EEG scalp topographies.

385 Besides identity coding, our findings also offer insights into the cortical coding of face sex.
386 As our stimulus set contained faces of opposite sexes, we could also track the emergence of sex
387 information. Face sex can be rapidly retrieved from EEG signals, both in univariate and
388 multivariate analyses, and predicts cortical organization from 140ms. This finding corroborates
389 previous ERP studies, which have suggested that face sex is extracted early and affects a variety
390 of face-related ERP components (Mouchetant-Rostaing et al., 2000; Ito and Urland, 2003, 2005;
391 Kloth et al., 2015). As opposed to the temporally sustained identity information, sex information
392 displayed a more transient nature, and vanished shortly before 700ms after onset. This difference
393 between identity and sex information suggests that the two properties are coded somewhat
394 independently at later processing stages.

395 In conclusion, we provide a characterization of the neural dynamics underlying familiar
396 face recognition. Representations of face identity emerged gradually across the visual processing
397 cascade. Invariant identity representations were observed after 400ms of processing. We suggest
398 that these representations are crucial for face recognition across different encounters with a
399 person.

400

References

Andrews S, Jenkins R, Cursiter H, Burton AM, Andrews S, Jenkins R, Cursiter H, Telling AMB, Andrews S, Jenkins R, Cursiter H, Burton AM (2015) Telling faces together : Learning new faces through exposure to multiple instances Telling faces together : Learning new faces through exposure to multiple instances. Q J Exp Psychol 0218:2041–2050 Available at: https://www.ncbi.nlm.nih.gov/pubmed/25607814.

Anzellotti S, Caramazza A (2014) The neural mechanisms for the recognition of face identity in humans. Front Psychol 5:672 Available at: https://www.ncbi.nlm.nih.gov/pmc/articles/PMC4072087/.

Anzellotti S, Fairhall SL, Caramazza A (2014) Decoding representations of face identity that are tolerant to rotation. Cereb Cortex 24:1988–1995 Available at: https://academic.oup.com/cercor/article-lookup/doi/10.1093/cercor/bht046.

Axelrod V, Yovel G (2015) Successful decoding of famous faces in the fusiform face area. PLoS One 10:e0117126 Available at: http://journals.plos.org/plosone/article?id=10.1371/journal.pone.0117126.

Bentin S, Deouell LY (2000) Structural Encoding and Identification in Face Processing: Erp Evidence for Separate Mechanisms. Cogn Neuropsychol 17:35–55 Available at: http://www.tandfonline.com/doi/abs/10.1080/026432900380472.

Besson G, Barragan-Jason G, Thorpe SJ, Fabre-Thorpe M, Puma S, Ceccaldi M, Barbeau EJ (2017) From face processing to face recognition: Comparing three different processing levels. Cognition 158:33–43 Available at: http://www.sciencedirect.com/science/article/pii/S0010027716302384.

Bruce V, Henderson Z, Greenwood K, Hancock PJB, Burton AM, Miller P (1999) Verification of face identities from images captured on video. J Exp Psychol Appl 5:339–360 Available at: http://psycnet.apa.org/fulltext/1999-01801-001.html.

Caharel S, Jiang F, Blanz V, Rossion B (2009) Recognizing an individual face: 3D shape contributes earlier

425 than 2D surface reflectance information. Neuroimage 47:1809–1818 Available at:
426 https://www.ncbi.nlm.nih.gov/pubmed/19497375.
427 Cichy RM, Kriegeskorte N, Jozwik KM, Bosch JJF van den, Charest I (2017) Neural dynamics of real-world
428 object vision that guide behaviour. bioRxiv:147298 Available at:
429 https://www.biorxiv.org/content/early/2017/06/08/147298.
430 Cichy RM, Pantazis D, Oliva A (2014) Resolving human object recognition in space and time. Nat Neurosci
431 17:455–462 Available at: https://www.nature.com/articles/nn.3635.
432 Cichy RM, Pantazis D, Oliva A (2016) Similarity-Based Fusion of MEG and fMRI Reveals Spatio-Temporal
433 Dynamics in Human Cortex During Visual Object Recognition. Cereb Cortex 26:3563–3579 Available
434 at: https://academic.oup.com/cercor/article/26/8/3563/2428700.
435 Clutterbuck R, Johnston RA (2002) Exploring levels of face familiarity by using an indirect face-matching
436 measure. Perception 31:985–994 Available at: https://www.ncbi.nlm.nih.gov/pubmed/12269591.
437 Curran T, Hancock J (2007) The FN400 indexes familiarity-based recognition of faces. Neuroimage
438 36:464–471 Available at: https://www.sciencedirect.com/science/article/pii/S1053811906011839.
439 Debruille JB, Guillem F, Renault B (1998) ERPs and chronometry of face recognition: following-up Seeck
440 et al. and George et al. Neuroreport 9:3349–3353 Available at:
441 http://www.ncbi.nlm.nih.gov/pubmed/9855278 [Accessed July 7, 2018].
442 Duchaine B, Yovel G (2015) A Revised Neural Framework for Face Processing. Annu Rev Vis Sci 1:393–416
443 Available at: http://www.annualreviews.org/doi/10.1146/annurev-vision-082114-035518.
444 Freeman JB, Ambady N, Holcomb PJ (2010) The face-sensitive N170 encodes social category information.
445 Neuroreport Available at: https://www.ncbi.nlm.nih.gov/pmc/articles/PMC3576572.
446 Gilaie-Dotan S, Malach R (2007) Sub-exemplar shape tuning in human face-related areas. Cereb Cortex
447 17:325–338 Available at: https://academic.oup.com/cercor/article-
448 pdf/17/2/325/17297436/bhj150.pdf.
449 Gobbini MI, Haxby J V. (2007) Neural systems for recognition of familiar faces. Neuropsychologia 45:32–

450 41 Available at: https://www.ncbi.nlm.nih.gov/pubmed/16797608.

451 Goesaert E, Op de Beeck HP (2013) Representations of Facial Identity Information in the Ventral Visual

452 Stream Investigated with Multivoxel Pattern Analyses. J Neurosci 33:8549–8558 Available at:

453 http://www.jneurosci.org/cgi/doi/10.1523/JNEUROSCI.1829-12.2013.

454 Gosling A, Eimer M (2011) An event-related brain potential study of explicit face recognition.

455 Neuropsychologia 49:2736–2745.

456 Gramfort A, Luessi M, Larson E, Engemann DA, Strohmeier D, Brodbeck C, Goj R, Jas M, Brooks T,

457 Parkkonen L, Hämäläinen M (2013) MEG and EEG data analysis with MNE-Python. Front Neurosci

458 Available at: https://www.frontiersin.org/articles/10.3389/fnins.2013.00267/full.

459 Gramfort A, Luessi M, Larson E, Engemann DA, Strohmeier D, Brodbeck C, Parkkonen L, Hämäläinen MS

460 (2014) MNE software for processing MEG and EEG data. Neuroimage 86:446–460 Available at:

461 https://www.ncbi.nlm.nih.gov/pubmed/24161808.

462 Groen IIA, Greene MR, Baldassano C, Fei-Fei L, Beck DM, Baker CI (2018) Distinct contributions of

463 functional and deep neural network features to representational similarity of scenes in human

464 brain and behavior. Elife 7 Available at: https://elifesciences.org/articles/32962.

465 Grootswagers T, Wardle SG, Carlson TA (2017) Decoding dynamic brain patterns from evoked responses:

466 A tutorial on multivariate pattern analysis applied to time series neuroimaging data. J Cogn

467 Neurosci 29:677–697 Available at:

468 https://www.mitpressjournals.org/doi/abs/10.1162/jocn_a_01068.

469 Heisz JJ, Watter S, Shedden JM (2006) Automatic face identity encoding at the N170. Vision Res 46:4604–

470 4614 Available at: https://www.sciencedirect.com/science/article/pii/S0042698906004573.

471 Huddy V, Schweinberger SR, Jentzsch I, Burton AM (2003) Matching faces for semantic information and

472 names: an event-related brain potentials study. Cogn Brain Res 17:314–326 Available at:

473 https://www.sciencedirect.com/science/article/pii/S0926641003001319 [Accessed July 7, 2018].

474 Ito TA, Urland GR (2003) Race and Gender on the Brain: Electrocortical Measures of Attention to the

475 Race and Gender of Multiply Categorizable Individuals. J Pers Soc Psychol 85:616–626 Available at:
476 https://www.ncbi.nlm.nih.gov/pubmed/14561116.
477 Ito TA, Urland GR (2005) The influence of processing objectives on the perception of faces: An ERP study
478 of race and gender perception. Cogn Affect Behav Neurosci 5:21–36 Available at:
479 https://www.ncbi.nlm.nih.gov/pubmed/15913005.
480 Jas M, Engemann DA, Bekhti Y, Raimondo F, Gramfort A (2017) Autoreject: Automated artifact rejection
481 for MEG and EEG data. Neuroimage 159:417–429 Available at:
482 https://doi.org/10.1016/j.neuroimage.2017.06.030.
483 Jenkins R, White D, Van Montfort X, Mike Burton A (2011) Variability in photos of the same face.
484 Cognition 121:313–323 Available at: https://www.ncbi.nlm.nih.gov/pubmed/21890124.
485 Jin J, Allison BZ, Kaufmann T, Kübler A, Zhang Y, Wang X, Cichocki A (2012) The Changing Face of P300
486 BCIs: A Comparison of Stimulus Changes in a P300 BCI Involving Faces, Emotion, and Movement
487 Frishman L, ed. PLoS One 7:e49688 Available at: http://dx.plos.org/10.1371/journal.pone.0049688
488 [Accessed July 7, 2018].
489 Johnston R a, Edmonds AJ (2009) Familiar and unfamiliar face recognition: a review. Memory 17:577–596
490 Available at: http://www.ncbi.nlm.nih.gov/pubmed/19548173.
491 Kaiser D, Oosterhof NN, Peelen M V. (2016) The Neural Dynamics of Attentional Selection in Natural
492 Scenes. J Neurosci 36:10522–10528 Available at:
493 http://www.jneurosci.org/cgi/doi/10.1523/JNEUROSCI.1385-16.2016.
494 Kloth N, Damm M, Schweinberger SR, Wiese H (2015) Aging affects sex categorization of male and
495 female faces in opposite ways. Acta Psychol (Amst) 158:78–86 Available at:
496 https://www.sciencedirect.com/science/article/pii/S0001691815000931 [Accessed July 7, 2018].
497 Kramer RSS, Young AW, Burton AM (2018) Understanding face familiarity. Cognition 172:46–58 Available
498 at: https://www.ncbi.nlm.nih.gov/pubmed/29232594.
499 Kriegeskorte N (2008) Representational similarity analysis – connecting the branches of systems

500 neuroscience. Front Syst Neurosci 2:4 Available at:
501 http://journal.frontiersin.org/article/10.3389/neuro.06.004.2008/abstract [Accessed July 7, 2018].
502 Kriegeskorte N, Formisano E, Sorger B, Goebel R (2007) Individual faces elicit distinct response patterns
503 in human anterior temporal cortex. Proc Natl Acad Sci 104:20600–20605 Available at:
504 http://www.pnas.org/cgi/doi/10.1073/pnas.0705654104.
505 Kriegeskorte N, Kievit RA (2013) Representational geometry: Integrating cognition, computation, and the
506 brain. Trends Cogn Sci 17:401–412 Available at:
507 https://www.ncbi.nlm.nih.gov/pmc/articles/PMC3730178/.
508 Liu J, Harris A, Kanwisher N (2013) Stages of processing in face perception: An MEG study. Soc Neurosci
509 Key Readings 5:75–86 Available at: http://www.nature.com/articles/nn909 [Accessed July 7, 2018].
510 Mike Burton A (2013) Why has research in face recognition progressed so slowly? The importance of
511 variability. Q J Exp Psychol 66:1467–1485 Available at:
512 http://www.ncbi.nlm.nih.gov/pubmed/23742022.
513 Mormann F, Kornblith S, Quiroga RQ, Kraskov A, Cerf M, Fried I, Koch C (2008) Latency and Selectivity of
514 Single Neurons Indicate Hierarchical Processing in the Human Medial Temporal Lobe. J Neurosci
515 28:8865–8872 Available at: http://www.jneurosci.org/cgi/doi/10.1523/JNEUROSCI.1640-08.2008.
516 Mouchetant-Rostaing Y, Giard MH, Bentin S, Aguera PE, Pernier J (2000) Neurophysiological correlates of
517 face gender processing in humans. Eur J Neurosci.
518 Nasr S, Tootell RBH (2012) Role of fusiform and anterior temporal cortical areas in facial recognition.
519 Neuroimage 63:1743–1753 Available at: https://www.ncbi.nlm.nih.gov/pubmed/23034518.
520 Natu V, O'Toole AJ (2011) The neural processing of familiar and unfamiliar faces: A review and synopsis.
521 Wiley/Blackwell (10.1111). Available at: http://doi.wiley.com/10.1111/j.2044-8295.2011.02053.x
522 [Accessed July 7, 2018].
523 Nemrodov D, Niemeier M, Mok JNY, Nestor A (2016) The time course of individual face recognition: A
524 pattern analysis of ERP signals. Neuroimage 132:469–476 Available at:

525 http://linkinghub.elsevier.com/retrieve/pii/S1053811916002020 [Accessed July 7, 2018].

526 Nemrodov D, Niemeier M, Patel A, Nestor A (2018) The Neural Dynamics of Facial Identity Processing:

527 insights from EEG-Based Pattern Analysis and Image Reconstruction. eneuro:ENEURO.0358-17.2018

528 Available at: http://eneuro.sfn.org/lookup/doi/10.1523/ENEURO.0358-17.2018 [Accessed July 7,

529 2018].

530 Nestor A, Plaut DC, Behrmann M (2011) Unraveling the distributed neural code of facial identity through

531 spatiotemporal pattern analysis. Proc Natl Acad Sci 108:9998–10003 Available at:

532 http://www.pnas.org/cgi/doi/10.1073/pnas.1102433108.

533 O'Toole AJ, Deffenbacher KA, Valentin D, McKee K, Huff D, Abdi H (1998) The perception of face gender:

534 The role of stimulus structure in recognition and classification. Mem Cogn 26:146–160 Available at:

535 https://www.ncbi.nlm.nih.gov/pubmed/9519705.

536 Oosterhof NN, Connolly AC, Haxby J V. (2016) CoSMoMVPA: Multi-Modal Multivariate Pattern Analysis of

537 Neuroimaging Data in Matlab/GNU Octave. Front Neuroinform 10:27 Available at:

538 http://journal.frontiersin.org/Article/10.3389/fninf.2016.00027/abstract [Accessed July 7, 2018].

539 Peirce JW (2008) Generating stimuli for neuroscience using PsychoPy. Front Neuroinform 2 Available at:

540 http://journal.frontiersin.org/article/10.3389/neuro.11.010.2008/abstract.

541 Quiroga RQ, Reddy L, Kreiman G, Koch C, Fried I (2005) Invariant visual representation by single neurons

542 in the human brain. Nature 435:1102–1107 Available at:

543 https://www.nature.com/articles/nature03687.

544 Rossion B, Hanseeuw B, Dricot L (2012) Defining face perception areas in the human brain: A large-scale

545 factorial fMRI face localizer analysis. Brain Cogn 79:138–157 Available at:

546 https://www.ncbi.nlm.nih.gov/pubmed/22330606.

547 Rossion B, Jacques C (2008) Does physical interstimulus variance account for early electrophysiological

548 face sensitive responses in the human brain? Ten lessons on the N170. Neuroimage 39:1959–1979

549 Available at: https://www.ncbi.nlm.nih.gov/pubmed/18055223.

Rossion B, Joyce CA, Cottrell GW, Tarr MJ (2003) Early lateralization and orientation tuning for face, word, and object processing in the visual cortex. Neuroimage 20:1609–1624 Available at: https://www.ncbi.nlm.nih.gov/pubmed/14642472.

Rousselet GA, Husk JS, Pernet CR, Gaspar CM, Bennett PJ, Sekuler AB (2009) Age-related delay in information accrual for faces: Evidence from a parametric, single-trial EEG approach. BMC Neurosci 10:114 Available at: http://bmcneurosci.biomedcentral.com/articles/10.1186/1471-2202-10-114 [Accessed July 7, 2018].

Schweinberger SR, Pickering EC, Jentzsch I, Burton AM, Kaufmann JM (2002) Event-related brain potential evidence for a response of inferior temporal cortex to familiar face repetitions. Cogn Brain Res 14:398–409 Available at: https://www.ncbi.nlm.nih.gov/pubmed/12421663.

Smith SM, Nichols TE (2009) Threshold-free cluster enhancement: Addressing problems of smoothing, threshold dependence and localisation in cluster inference. Neuroimage 44:83–98 Available at: https://www.ncbi.nlm.nih.gov/pubmed/18501637.

Tanaka JW, Curran T, Porterfield AL, Collins D (2006) Activation of Preexisting and Acquired Face Representations: The N250 Event-related Potential as an Index of Face Familiarity. J Cogn Neurosci 18:1488–1497 Available at: http://www.mitpressjournals.org/doi/10.1162/jocn.2006.18.9.1488 [Accessed July 7, 2018].

Verosky SC, Todorov A, Turk-Browne NB (2013) Representations of individuals in ventral temporal cortex defined by faces and biographies. Neuropsychologia 51:2100–2108 Available at: https://www.ncbi.nlm.nih.gov/pubmed/23871881.

Vida MD, Nestor A, Plaut DC, Behrmann M (2017) Spatiotemporal dynamics of similarity-based neural representations of facial identity. Proc Natl Acad Sci 114:388–393 Available at: http://www.pnas.org/lookup/doi/10.1073/pnas.1614763114 [Accessed July 7, 2018].

Visconti Di Oleggio Castello M, Halchenko YO, Guntupalli JS, Gors JD, Gobbini MI (2017) The neural representation of personally familiar and unfamiliar faces in the distributed system for face

perception. Sci Rep 7:12237 Available at: http://www.nature.com/articles/s41598-017-12559-1 [Accessed July 7, 2018].

Wang Z, Bovik AC, Sheikh HR, Simoncelli EP (2004) Image quality assessment: From error visibility to structural similarity. IEEE Trans Image Process 13:600–612 Available at: https://ieeexplore.ieee.org/document/1284395.

Weibert K, Andrews TJ (2015) Activity in the right fusiform face area predicts the behavioural advantage for the perception of familiar faces. Neuropsychologia 75:588–596 Available at: https://www.ncbi.nlm.nih.gov/pubmed/26187507.

Weibert K, Harris RJ, Mitchell A, Byrne H, Young AW, Andrews TJ (2016) An image-invariant neural response to familiar faces in the human medial temporal lobe. Cortex 84:34–42 Available at: https://www.ncbi.nlm.nih.gov/pubmed/27697662.

Young AW, Burton AM (2017) Recognizing Faces. Curr Dir Psychol Sci 26:212–217 Available at: journals.sagepub.com/doi/abs/10.1177/0963721416688114.

Yovel G (2016) Neural and cognitive face-selective markers: An integrative review. Neuropsychologia 83:5–13 Available at: https://www.ncbi.nlm.nih.gov/pubmed/26407899.

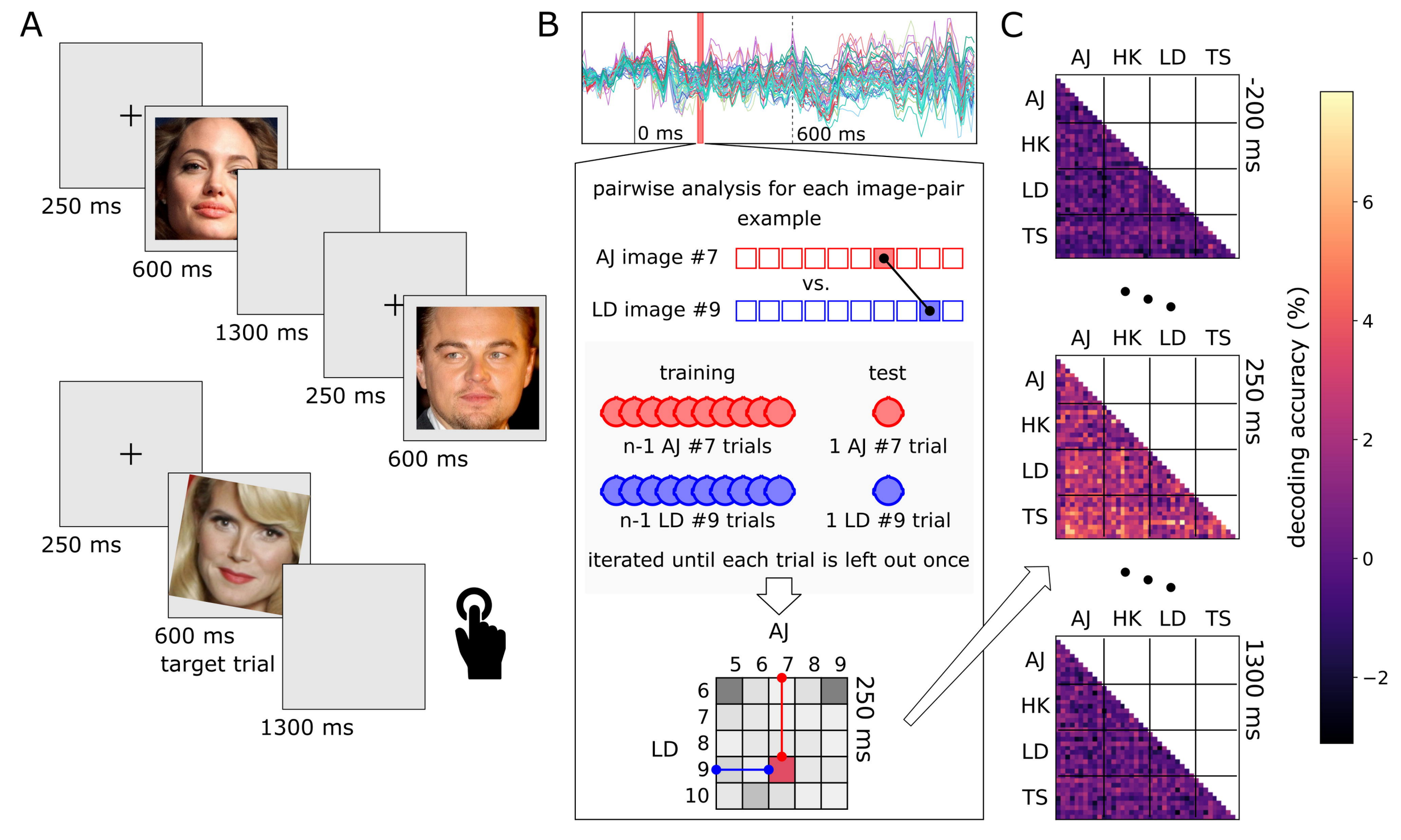
A
250 ms
600 ms
1300 ms
250 ms
600 ms
250 ms
600 ms
target trial
1300 ms
B
0 ms
600 ms
pairwise analysis for each image-pair
example
AJ image #7
vs.
LD image #9
training
test
n-1 AJ #7 trials
1 AJ #7 trial
n-1 LD #9 trials
1 LD #9 trial
iterated until each trial is left out once
AJ
5 6 7 8 9
6
7
8
9
10
LD
250 ms
C
AJ HK LD TS
AJ
HK
LD
TS
-200 ms
250 ms
1300 ms
decoding accuracy (%)
6
4
2
0
−2

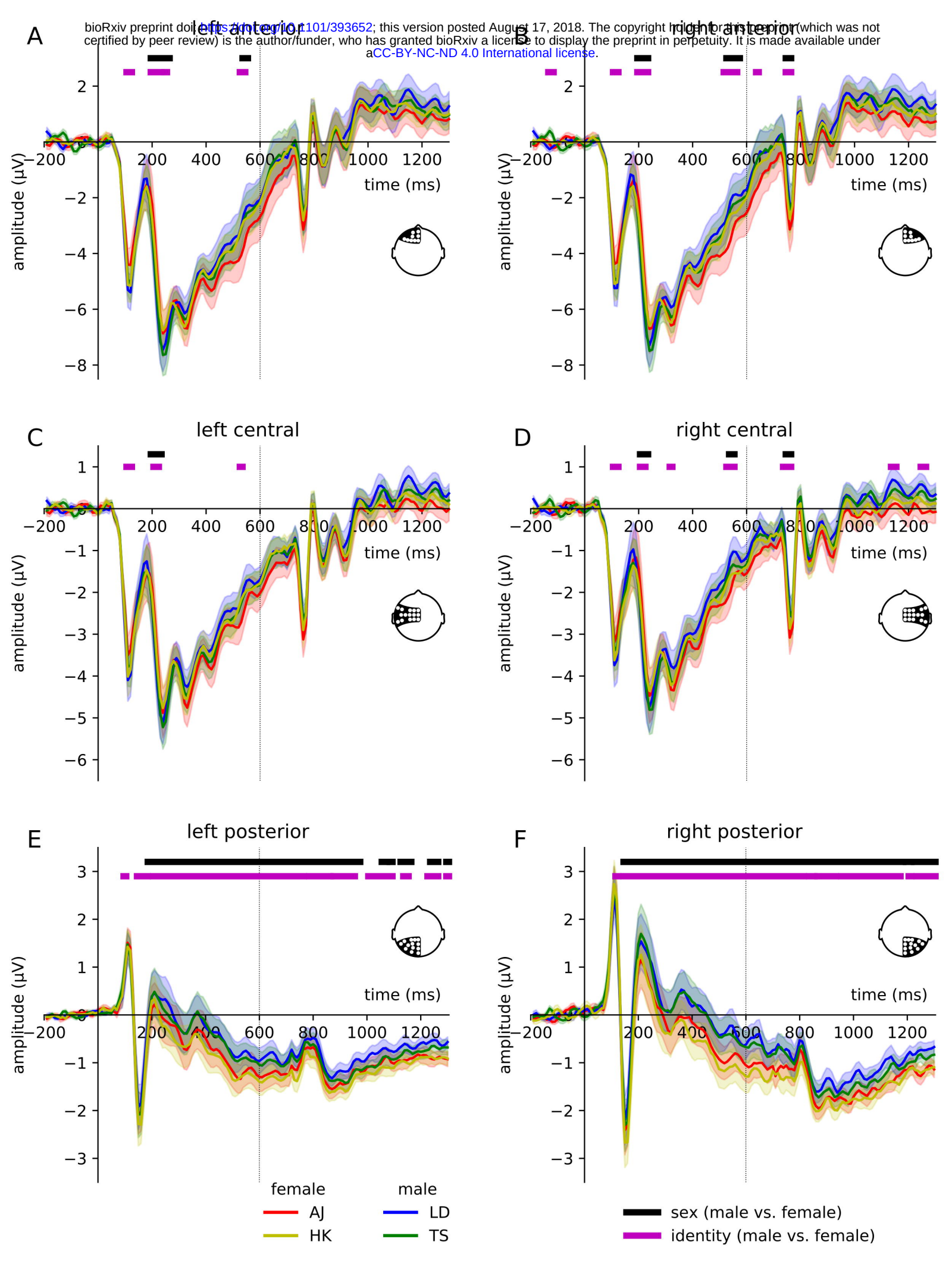

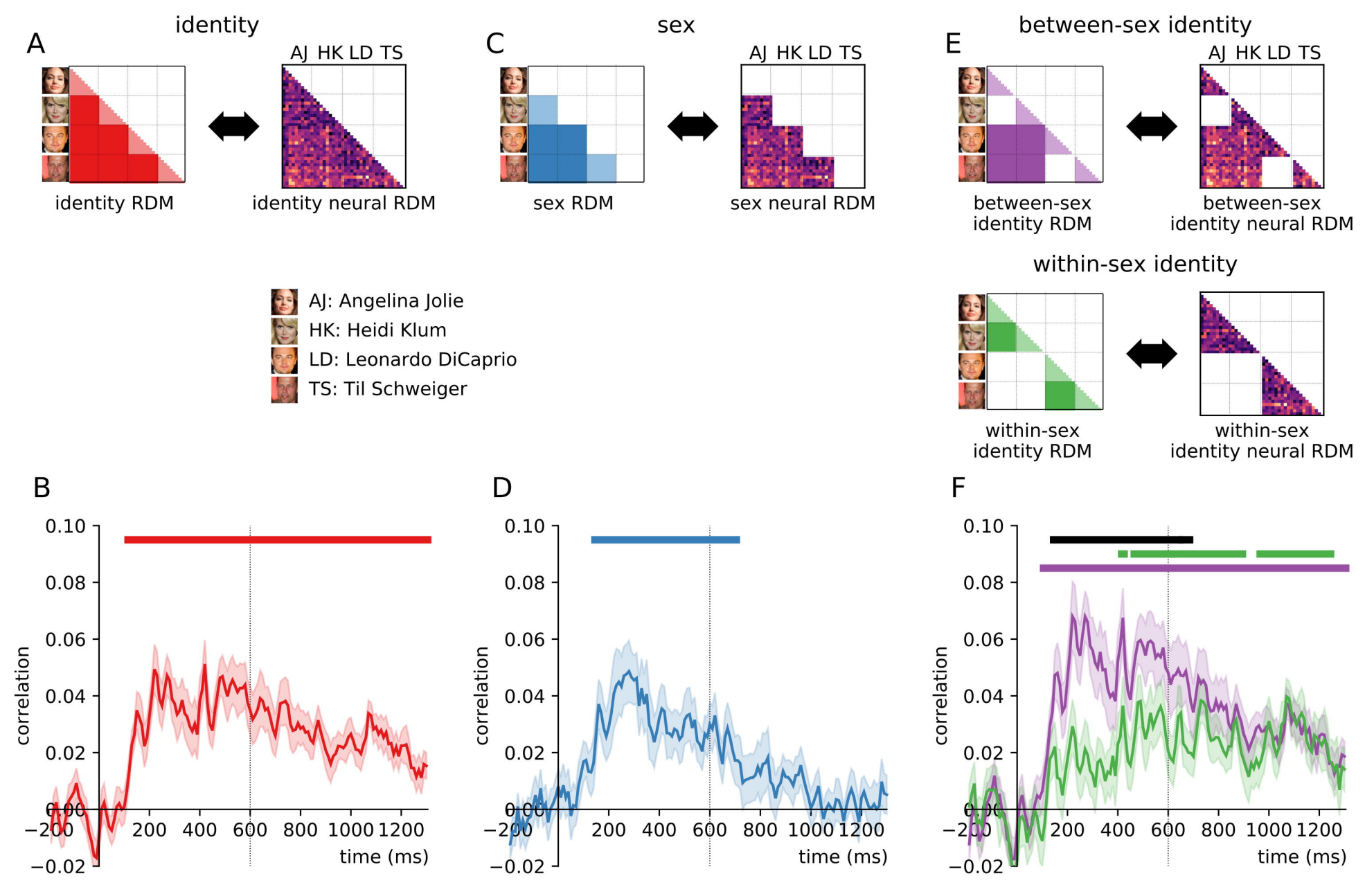
A
identity
AJ HK LD TS
identity RDM
identity neural RDM
C
sex
AJ HK LD TS
sex RDM
sex neural RDM
E
between-sex identity
AJ HK LD TS
between-sex identity RDM
between-sex identity neural RDM
within-sex identity
within-sex identity RDM
within-sex identity neural RDM
AJ: Angelina Jolie
HK: Heidi Klum
LD: Leonardo DiCaprio
TS: Til Schweiger
B
D
F
correlation
time (ms)
0.10
0.08
0.06
0.04
0.02
0.00
−0.02
−200
200
400
600
800
1000
1200

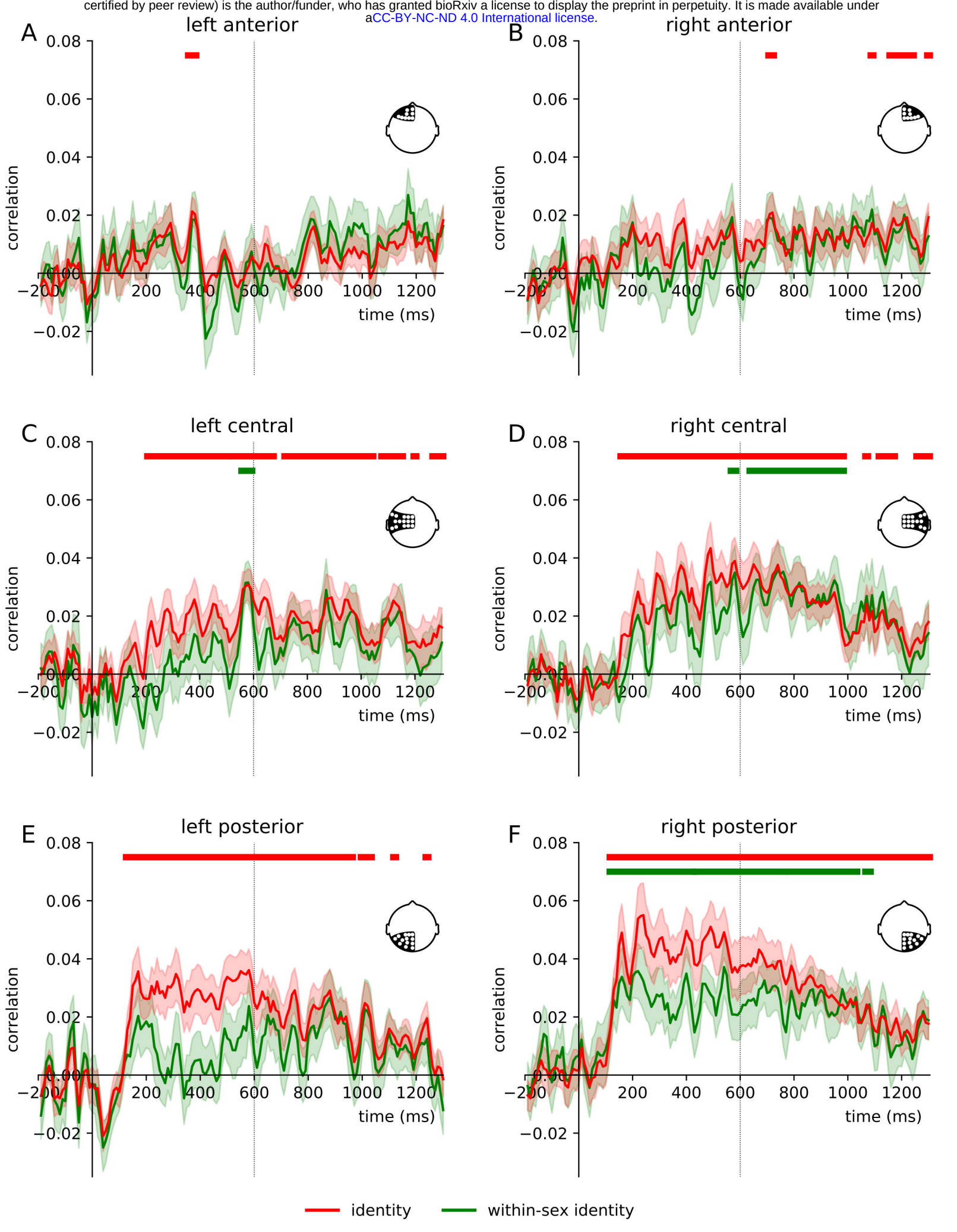

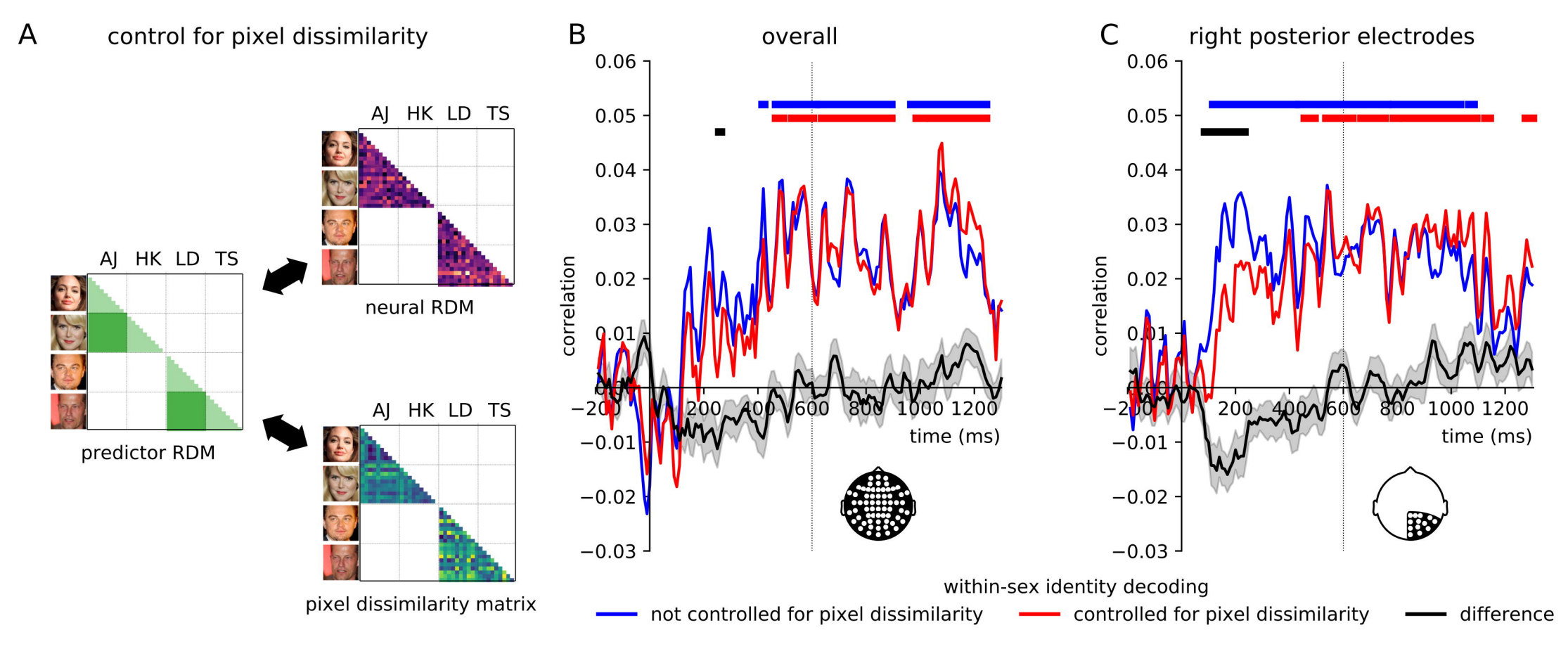
A
control for pixel dissimilarity
AJ HK LD TS
AJ HK LD TS
neural RDM
predictor RDM
AJ HK LD TS
pixel dissimilarity matrix
B
overall
C
right posterior electrodes
correlation
time (ms)
0.06
0.05
0.04
0.03
0.02
0.01
−0.01
−0.02
−0.03
200
400
600
800
1000
1200
within-sex identity decoding
not controlled for pixel dissimilarity
controlled for pixel dissimilarity
difference